Cancer Cell International

RESEARCH

Open Access

FBXL18 promotes endometrial carcinoma progression via destabilizing DUSP16 and thus activating JNK signaling pathway

Jie Pi[1], Yong Wang[1], Yuzi Zhao[1] and Jing Yang[1*]

Abstract

Objective The therapeutic options for patients with advanced endometrial carcinoma (EC) were still limited and the prognosis remained unfavorable. F-box and leucine-rich repeat protein 18 (FBXL18), belonging to the F-box protein family, was frequently altered in human cancer, while its functional role and underlying mechanisms in EC were largely unexplored.

Methods The expression of FBXL18 in EC tissues and cells were explored using data mining strategies and further experiments. Multiple in *vitro* assays, including CCK-8, colony formation, wound healing, and Transwell invasion assays, were performed to assess the function of FBXL18 on cell proliferation, migration, and invasion. Bioinformatic analyses, western blot, qRT-PCR, Co-immunoprecipitation and ubiquitination assays were employed to identify the downstream pathway and direct substrate of FBXL18.

Results FBXL18 was highly expressed in EC tissues and cell lines, and EC patients with high FBXL18 expression had poor clinical outcome. Loss- and gain-of-function assays showed that silencing FBXL18 suppressed EC cell proliferation, migration, and invasion, while overexpressing FBXL18 caused the opposite effects. Mechanistically, FBXL18 could physically interacted with DUSP16, a dual specificity phosphatase, leading to its ubiquitination and degradation, and thus activating JNK signaling pathway. Upregulation of DUSP16 in EC cells alleviated FBXL18 overexpression-induced activation of JNK signaling pathway, and reversed FBXL18 overexpression-mediated enhanced cell capacities of proliferation, migration, and invasion.

Conclusion In summary, our study had showcased the elevated expression, prognostic prediction performance, and the malignant tumor-promoting role of FBXL18 in EC. The novel mechanisms underlying this phenotype are that FBXL18 promotes the ubiquitination and degradation of DUSP16, and thus activates JNK/c-JUN signaling to facilitate EC progression.

Keywords FBXL18, Endometrial carcinoma, DUSP16, JNK signaling, Ubiquitination

*Correspondence:
Jing Yang
dr_yangjing2023@163.com
[1]Department of Obstetrics and Gynecology, Renmin Hospital of Wuhan University, Wuhan 430060, China

Introduction

Endometrial carcinoma (EC), a kind of epithelial tumor, was arising from the endometrial epithelial tissues and was one of the most common gynecologic malignant tumors in developed countries [1, 2]. EC was the sixth most common tumors in women worldwide, posing a huge health burden to the human beings [3]. It was estimated that there were approximately 417,367 new cases of EC in 2020, and about 97,370 cases among women dies from EC [4, 5], with the morbidity and mortality rates were increasing in the last years. EC often occurred in elderly women, with a median age at diagnosis of 61 years [6]. However, recent clinical experiments suggested a trend of younger onset of EC patients. Nowadays, great progress had been made in the treatment strategies including surgical resection, postoperative chemoradiotherapy, and radiotherapy for EC patients [7, 8], which were effective in cases of early stage, with a 5-year survival rate reaching about 85% [9]. The therapeutic options for patients with advanced EC were still limited and the prognosis remained unfavorable [10, 11]. Thus, it was urgent to explore the driver genes of EC occurrence and progression, which might lead to the identification of potential therapeutic targets for EC patients.

F-box and leucine-rich repeat protein 18 (FBXL18) belongs to the F-box protein family. Members of this protein family contain F-box motif, which was previously reported to function as indispensable substrate-recognition subunits and recruit proteins to the SKP1- Skp1-Cullin1-F-box (SCF) ubiquitin ligase complex [12, 13]. F-box proteins were frequently altered in many human diseases including cancer, and might be promising therapeutic targets due to their vital roles in regulating multiple important signaling pathways such as Hedgehog, WNT, MAPK, and NF-κB [14–17]. Previous studies had revealed the aberrant expression of F-box proteins in various cancers, and their dual roles that either served as tumor promoting factor or tumor suppressor, depending on tumor types [18, 19]. For example, Yu et al. [20]. reported that FBXL18 was highly expressed in hepatocellular carcinoma (HCC) and predicted poor overall survival for HCC patients. Functionally, elevated expression of FBXL18 promoted HCC cell proliferation in *vitro*, and driven HCC progression in transgenic mice. Further exploration revealed that FBXL18 increased the stability of RPS15A via promoting its K63-linked ubiquitination, leading to the activation of SMAD3 signaling. *Yoshida et al.* [21]. showed that FBXL8 suppressed lymphoma growth by promoting the degradation of phosphorylated cyclin D3. Despite these findings, the expression level, functional role and underlying mechanisms of FBXL18 in EC remained largely unexplored.

In this study, we showed that FBXL18 was aberrantly expressed in EC tissues and cell lines using data mining strategies and further experiments. We found that EC patients with high FBXL18 expression harbored poor prognosis. Then, the data of loss- and gain-of-function assays revealed that FBXL18 knockdown reduced cell capacities of proliferation, migration, and invasion in EC, while enforced FBXL18 expression led to opposite effects. Mechanistically, FBXL18 could physically interact with DUSP16, a dual specificity phosphatase, leading to its ubiquitination and degradation, and thus activating JNK signaling pathway. In summary, our study had identified a unique regulatory pathway involving FBXL18-DUSP16-JNK axis, which could effectively control malignant behaviors of EC cells. The FBXL18-DUSP16-JNK axis might be an attractive therapeutic target for the treatment of EC.

Materials and methods

Data acquisition

We downloaded RNA sequencing data and related clinical information from endometrial Cancer (UCEC) samples from The Cancer Genome Atlas (TCGA) database. Data standardization was performed using Fragments Per Kilobase Million (FPKM) to ensure comparability of expression levels.

Sample collection

Endometrial carcinoma samples ($n = 12$) and paired normal tissues ($n = 12$) were obtained from patients who underwent surgery in the Department of Gynecology and Obstetrics, Renmin Hospital of Wuhan University, from January 2021 to December 2023. All patients were pathologically diagnosed as endometrial cancer by two independent pathologists. All samples were immediately frozen in liquid nitrogen after resection, and stored in -80 °C until being used for further analyses. The collection and use of these clinical specimens were approved by the Ethical Committee of the Renmin Hospital of Wuhan University, with written informed permission from each patient or their legal guardian.

Cell lines and cell culture

The normal endometrial stromal cell line (ESC) and EC cell lines (KLE, Ishikawa) were purchased from Pricella Biotechnology (Wuhan, China). The EC cell lines (HEC-1B, RL95-2) and HEK 293T cells were obtained from the Cell Bank of the Chinese Scientific Academy (Shanghai, China). All cell lines were cultured in DMEM (Hyclone, USA) containing 10% fetal bovine serum (FBS; Beyotime, Shanghai, China), except for KLE and RL95-2 cells, which were maintained in DMEM/F12 (Hyclone, USA) with 10% FBS. All cells were kept in a humidified cell incubator at 37 °C with a 5% CO2 environment.

Lentivirus, plasmids, SiRNA, and generation of stably cell lines

Lentivirus containing shRNA targeting FBXL18 (shFBXL18) or negative control shRNA (shNC), and FBXL18-overexpressing plasmid (LV-FBXL18) or empty vector (LV-Control), were all purchased from Gene Pharma Company (Shanghai, China). Full-length human FLAG-tagged FBXL18 and HA-tagged DUSP16 were inserted into pcDNA.3.1 plasmids to generate tagged proteins. SiRNA specifically targeting DUSP16 or negative control siRNA (siNeg) were obtained from Sangon Biotech (Shanghai, China). To generate stably cell lines, cells were seeded in 6-well plates and cultured to reach a cellular confluence of 50%. Then, cells were incubated with indicated lentivirus according to the manufacturer's protocol. The stably infected cells were screened out by exposing to puromycin (3 μg/ml) for one week. For siRNA or plasmid transfection, HighGene reagent (ABclonal, Wuhan, China) was employed following the manufacturer's instructions. The knockdown or overexpression of target genes were confirmed at both mRNA and protein levels by performing qRT-PCR and western blot assays.

Cell proliferation assays

Cell proliferation ability was examined by CCK-8 and colony formation assays. For CCK-8 assay, cells of the indicated groups were seeded into 96-well plates at a density of 5×10^3 cells per well. After culturing for 0, 24, 48, and 72 h, CCK-8 reagents (Beyotime, Shanghai, China) were added into specified wells. Following a 1 h incubation at 37 °C in dark, the optical density (OD) values at 450 nm were measured using a microplate reader. For colony formation assay, different groups of equal cells (1×10^3/well inoculated in shNC, shFBXL18, LV-Control and LV-FBXL18) were placed in 6-well plates and in humidified cell incubators under standard circumstance. The supernatants were replaced with fresh complete medium every five days. After about two weeks, cells were washed with cold PBS for 5 min twice, and then fixed in 4% paraformaldehyde (Servicebio, Wuhan, China) for 15 min at room temperature. Subsequently, cells were stained with 1% crystal violet (Beyotime, Shanghai, China) for 20 min, followed by washing with PBS for 10 min twice. The visible colonies were observed and photographed. The numbers of colonies in each group were counted using ImageJ software. In this experiment, we defined a cell cluster composed of 50 or more cells as a clonal colony.

Wound healing and transwell invasion assay

Cell motility capacity was evaluated by wound healing and Transwell invasion assays. In the wound healing assay, cells of each group were seeded into 6-well plates and cultured in complete media to reach a 95% coverage. Then, a straight wound was made in the bottom of each well using a 200 μl pipette tip. Cells were washed with PBS, and cultured in serum-free media for another 24 h. The areas of wound in each well at 0 and 24 h were observed and photographed under an inverted microscope (Olympus, Japan). The wound healing rate was determined using the following formula: Wound healing rate = (initial wounded area - remained wound area) / initial wounded area × 100%. For Transwell invasion assay, cells of different groups were resuspended in the corresponding serum-free media at a density of 5×10^5/ml. A total of 1×10^4 cells in 200 μl media were introduced into the upper wells of the Transwell chambers (Corning, USA), which were pre-coated with Matrigel solution (BD, USA). The lower wells of the Transwell chambers were supplemented with 600 μl media containing 20% FBS. After incubating for 36 h at standard circumstance, cells invading to the lower surface of the Transwell chambers were fixed with 4% paraformaldehyde for 30 min, while cells in the upper of the Transwell chambers were removed by a cotton swab. Subsequently, the invaded cells were stained with 1% crystal violet, followed by being washed with PBS twice. Five representative microscopic fields were observed and photographed under an inverted microscope (Olympus, Japan). The number of invaded cells of each group was determined using ImageJ software.

RNA isolation and qRT-PCR

Total RNAs were isolated from cultured cells and tissues using TRIzol reagent (Invitrogen, USA) according to the instruction. After measuring the concentration of total RNAs, one microgram of RNAs were reversely transcribed into cDNAs with BeyoRT II M-MLV reverse transcriptase (Beyotime, Shanghai, China). Quantitative real-time PCR analysis was performed on a LightCycler 480 system (Roche, Germany) using SYBR Green (Takara, Beijing, China) following the standard protocol. The relative gene expression level was calculated using $2^{-\Delta\Delta CT}$ method, and the housekeeping gene *GAPDH* was employed for normalization. All the primers were obtained from Sangon Biotech (Shanghai, China), and the sequences of primers were listed as follow: *GAPDH*, 5'-CCAAGGAGTAAGACCCCTGG-3' (forward), 5'-TGGTTGAGCACAGGGTACTT-3' (reverse); *FBXL18*, 5'-CTGTTCACTCCCTCCTACGG-3' (forward), 5'-TAAGCACAGCCAGGTAGAGC-3' (reverse); *DUSP16*, 5'-CGAAGGTTGCAACAGGACAA-3' (forward), 5'-GAACTCAGCAAACCCACCTG-3' (reverse).

Protein extraction and western blotting

RIPA lysis buffer (Solarbio, Beijing, China), supplemented with 1% phosphatase and protease inhibitors (Servicebio, Wuhan, China), was used for protein extraction from cultured cells and tissues. The protein

concentration was measured with BCA kit (Solarbio, Beijing, China) following standard protocol. After normalizing protein concentration of each sample to 1 μg/μl with RIPA lysis buffer and loading buffer, a total of 15 μg proteins were subjected to 10% SDS polyacrylamide gels, followed by being transferred into the PVDF membranes (Millipore, USA). Subsequently, the membranes were blocked with 5% nonfat milk at room temperature for 1 h and then incubated with specific primary antibodies at 4 °C overnight. The next day, membranes were washed with Tris-buffered saline with Tween 20 (TBST) twice and then incubated with horseradish peroxidase (HRP)-conjugated secondary antibodies at room temperature for 2 h. The protein bands were finally visualized using enhanced chemiluminescence reagent (Beyotime, Shanghai, China). GAPDH protein level was employed for normalization, and the relative protein expression level was determined by ImageJ software. The primary antibodies included FBXL18 (sc-100738, Santa Cruz, USA; 1:500), DUSP16 (#5523, CST, USA; 1:1000), GAPDH (GB15004-100, Servicebio, China; 1:500), JNK (#9252, CST, USA; 1:1000), p-JNK (#9251, CST, USA; 1:500), c-Jun (#9165, CST, USA; 1:1000), and p-c-Jun (#3270, CST, USA; 1:1000).

Co-immunoprecipitation (Co-IP) and ubiquitination assay

Briefly, cells of the indicated groups were collected and then lysed in cold IP lysis buffer. Subsequently, specific primary antibodies were added into the protein lysate, followed by rotating gently at 4 °C overnight. The next day, the resultant mixtures were incubated with the pre-treated protein A + G agarose beads (CST, USA) at 4 °C with gently rotation for 2 h. After centrifuging at 2000 rpm for 5 min, the supernatant was discarded and the precipitates were collected for subsequent western blot analysis. The primary antibodies included FBXL18 (sc-100738, Santa Cruz, USA), DUSP16 (#5523, CST, USA), FLAG (#14793, CST, USA), HA (#3724, CST, USA). For the in vivo ubiquitination assay, cells were of different groups were treated with MG132 (20 μM; MCE, USA) for 6 h before collection. Then, total proteins were isolated in IP lysis buffer and immunoprecipitated with DUSP16 antibody. Anti-Ub (ABclonal, Wuhan, China) antibody were utilized for western blot analysis.

Protein stability and degradation experiment

Protein stability and degradation were assessed by performing cycloheximide-chase degradation assay. Briefly, cells of different groups were seeded in 6-well plates and cultured to reach a density of approximately 80%. Then, cells were treated with cycloheximide (10 μg/ml; MCE, USA) for 0, 2, 4, and 8 h. At the indicated time points, cells were harvest for protein extraction and further western blot analysis.

Animal experiments

Briefly, KLE cells stably transfected with lentivirus containing shRNA targeting FBXL18 (shFBXL18) or control shRNA (shNC) were harvest and resuspended in PBS at a density of 5×10^7/ml. A total of 100 μl cell suspension were mixed with Matrigel at a ratio of 1:1, and were then subcutaneously injected into the lower dorsal surface of female BALB/c nude mice ($n = 6$; six weeks old, male, obtained from HFK Bioscience (Beijing, China)). Tumor volume was monitored every week and determined by measuring the visible xenograft in two perpendicular directions. Five weeks post injection, all the mice were euthanized. The xenograft tumors were resected and weighted, as well as being photographed. Then, all the samples were divided into two parts: one was being fixed in 4% paraformaldehyde, and the other part were being frozen and stored in liquid nitrogen for further analysis.

Statistically analysis

R 4.1.0 software and GraphPad Prism 8 were employed for data analysis and visualization. All data were presented as the mean ± standard deviations (SDs). Differences between two or multiple groups were compared by unpaired Student's *t*-test or one-way analysis of variance (ANOVA). Kaplan-Meier (KM) plot and log-rank test was used for the comparison of overall survival between different groups. A *P*-value less than 0.05 was considered as statistically significant. Significance levels $^{*}P < 0.05$; $^{**}P < 0.01$; $^{***}P < 0.001$.

Results

FBXL18 was highly expressed in EC tissues and cells, and augmented expression predicted poor prognosis

We first evaluated FBXL18 expression in Pan-cancers using the TIMER platform (https://cistrome.shinyapps.io/timer/). As shown in Fig. 1A, when comparing to co rresponding normal tissues, FBXL18 mRNA levels were markedly higher in tumors including Bladder Urothelial Carcinoma (BLCA), Cholangiocarcinoma (CHOL), Colon adenocarcinoma (COAD), Esophageal carcinoma (ESCA), Head and Neck squamous cell carcinoma (HNSC), Kidney Chromophobe (KICH), Liver hepatocellular carcinoma (LIHC), Lung adenocarcinoma (LUAD), Lung squamous cell carcinoma (LUSC), Prostate adenocarcinoma (PRAD), Rectum adenocarcinoma (READ), Stomach adenocarcinoma (STAD), and Uterine Corpus Endometrial Carcinoma (UCEC), while FBXL18 expression was downregulated in Kidney renal clear cell carcinoma (KIRC) and Kidney renal papillary cell carcinoma (KIRP). These results suggested that FBXL18 was frequently dysregulated in tumors and might participated in tumorigenesis and progress. Then, data from the online public databases UALCAN (https://ualcan.path.uab.edu/index.html) showed that FBXL18 was upregulated more

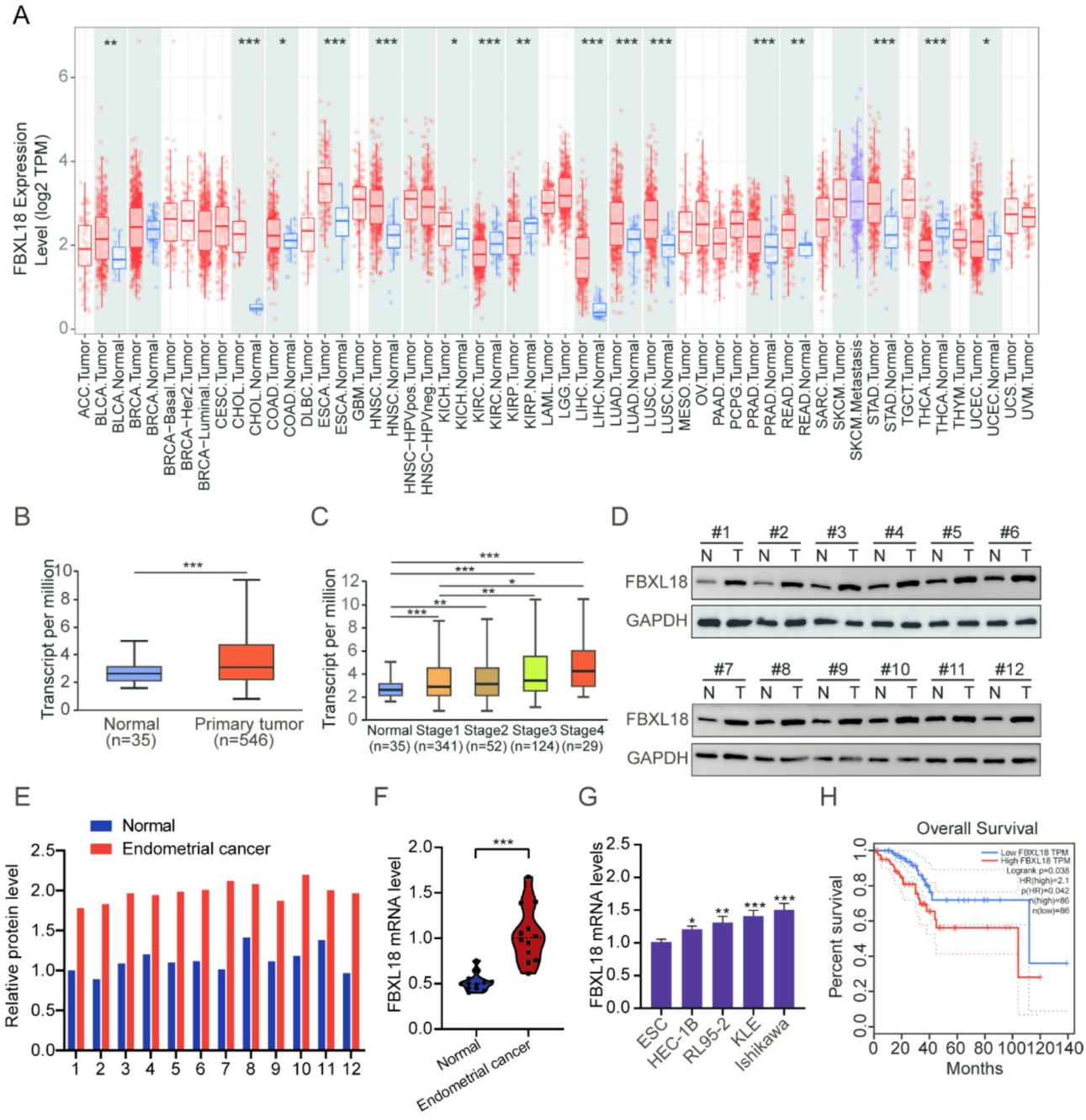

Fig. 1 FBXL18 was highly expressed in EC tissues and cells, and augmented expression predicted poor prognosis. (**A**) The expression of FBXL18 in various tumors from the TIMER database. (**B**) The mRNA expression pattern of FBXL18 in EC tissues and corresponding normal tissues was analyzed using the UALCAN database. (**C**) The comparison of FBXL18 mRNA level in normal tissues and EC tissues of different tumor stage. (**D-E**) Western blot analysis of FBXL18 protein levels in twelve pairs of EC tissues and adjacent normal tissues, and quantitative analysis. (**F**) qRT-PCR analysis of FBXL18 mRNA levels in twelve paired EC tissues and adjacent normal tissues. (**G**) qRT-PCR analyses of FBXL18 mRNA levels in normal endometrial stromal cells (ESC) and a variety of EC cells (KLE, Ishikawa, HEC-1B, RL95-2). (**H**) The association of FBXL18 expression and patients' overall survival was determined. *$P<0.05$; **$P<0.01$; ***$P<0.001$

in EC tissues than in adjacent normal tissues (Fig. 1B), and FBXL18 expression exhibited a trend to be elevated with the increase of tumor stage (Fig. 1C). The results of western blot and qRT-PCR assays in twelve pairs of EC tissues and adjacent nontumor tissues showed the protein and mRNA levels of FBXL18 were consistently higher in EC tissues (Fig. 1D-F). Similarly, qRT-PCR analysis performed on EC cell lines and normal endometrial stromal cell line (ESC) revealed considerably higher FBXL18 expression in multiple EC cell lines (KLE, Ishikawa,

HEC-1B, RL95-2) compared to ESC (Fig. 1G). Moreover, we stratified EC patients into high- and low-expression groups based on median expression level of FBXL18, and the subsequent Kaplan-Meier survival analysis revealed that patients with elevated FBXL18 levels harbored poor overall survival (Fig. 1H). Taken together, these results illustrated that FBXL18 was highly expressed in EC, and the upregulation of FBXL18 was associated with poor prognosis in EC patients.

Silence of FBXL18 impeded cell proliferation, migration, and invasion, and suppressed EMT in EC cells

We further assessed the role of FBXL18 in the malignant biological behavior of EC by using specific shRNA targeting FBXL18 to delete endogenous FBXL18 expression in KLE and Ishikawa cells. qRT-PCR and western blot assays confirmed a significant inhibition of FBXL18 mRNA and protein levels in EC cells of shFBXL18 group than that in shNC group (Fig. 2A-C). In the CCK-8 and colony formation assays, we observed that the optical density (OD) values and number of colonies were markedly reduced in shFBXL18 group compared to that in shNC group (Fig. 2D-G), suggesting decreased cell proliferation capacity after silencing FBXL18. Subsequently, in the Transwell invasion and wound healing assays, our results illustrated that silence of FBXL18 could effectively inhibit the invasion and migration abilities of KLE and Ishikawa cells, as evidenced by reduced number of invaded cells and decreased cell migration rates in shFBXL18 group (Fig. 2H-L). Epithelial-mesenchymal transformation (EMT) was a tightly regulated process, in which cells lose their epithelial characteristics and acquire mesenchymal features. It had been reported to be closely related to EC initiation, progression, metastasis [22]. Therefore, we evaluated the effect of FBXL18 on EMT process in EC cells by detecting the protein levels of EMT-related biomarkers. The results of western blot assay suggested the protein levels of mesenchymal markers (N-cadherin, Vimentin) were significantly downregulated, while the protein level of the epithelial markers (E-cadherin) was upregulated, in the shFBXL18 group compared with that in shNC group (Fig. 2M-O), indicating decreased EMT features after silencing FBXL18 in EC cells. In all, these results demonstrated that silence of FBXL18 suppressed cell proliferation, migration, and invasion, and impeded EMT process in EC cells.

Enforced expression of FBXL18 accelerated cell proliferation, migration, and invasion, and promoted EMT in EC cells

To further evaluate the role of FBXL18 in EC cells, we also established stably cell lines overexpressing FBXL18 through lentivirus-mediated plasmid transfection method. Notably, the mRNA and protein levels of FBXL18 in KLE and Ishikawa cells were markedly increased in LV-FBXL18 group compared to that in LV-Control group, as evidenced by the results of qRT-PCR and western blot assays (Fig. 3A-C). This intervention led to enhanced optical density (OD) values and increased colony numbers in the CCK-8 and colony formation assays, respectively (Fig. 3D-G), suggesting accelerated cell proliferation after overexpressing FBXL18. Further analyses using Transwell invasion and wound healing assays revealed that enforced expression of FBXL18 significantly increased cell invasiveness and motility (Fig. 3H-L). Western blot assay was also employed to assess the effect of FBXL18 on EMT process of EC cells. The results showed that overexpression of FBXL18 observably increased the protein levels of mesenchymal markers (N-cadherin, Vimentin), and decreased the protein level of epithelial markers (E-cadherin) (Fig. 3M-O). Collectively, these data provided evidence that FBXL18 acted as a promoting factor in modulating the oncogenic phenotypes of EC cells.

FBXL18 positively regulated JNK signaling pathway in EC

To thoroughly explore the underlying molecular regulatory mechanism of FBXL18, we employed The Cancer Genome Atlas (TCGA) database to gather RNA sequencing data of EC samples. We first calculated the median value of FBXL18 expression in all samples. The samples were then divided into two groups based on the median: High expression group: samples with higher than median FBXL18 expression levels. Low expression group: Samples with FBXL18 expression levels below or equal to the median. As shown in Fig. 4A, a total of 1302 differentially expressed genes (DEGs) between $FBXL18^{High}$ and $FBXL18^{Low}$ groups were identified, with 557 upregulated and 745 downregulated genes in $FBXL18^{High}$ group when comparing to that in $FBXL18^{Low}$ group. Subsequently, these FBXL18-related DEGs were subjected to GO and KEGG enrichment analyses. In the biological process category, single-organism process, multicellular organismal process, and single – multicellular organism process were the three most enriched terms. As for the cellular component, these DEGs were mainly involved in extracellular region, extracellular region part, and extracellular space. With respect to molecular function, DEGs particularly took part in channel activity, substrate-specific channel activity, and serine hydrolase activity (Fig. 4B). In the KEGG enrichment analysis, multiple tumor-related pathways including MAPK, cAMP, PI3K-Akt, Ras, Estrogen, and cGMP-PKG signaling pathways, were highly enriched (Fig. 4C). Furthermore, GSEA results revealed that MAPK signaling pathway and ubiquitin-mediated proteolysis were markedly enriched in $FBXL18^{High}$ group (Fig. 4D-E). Moreover, Pearson's correlation analysis illustrated that *FBXL18* expression was positively

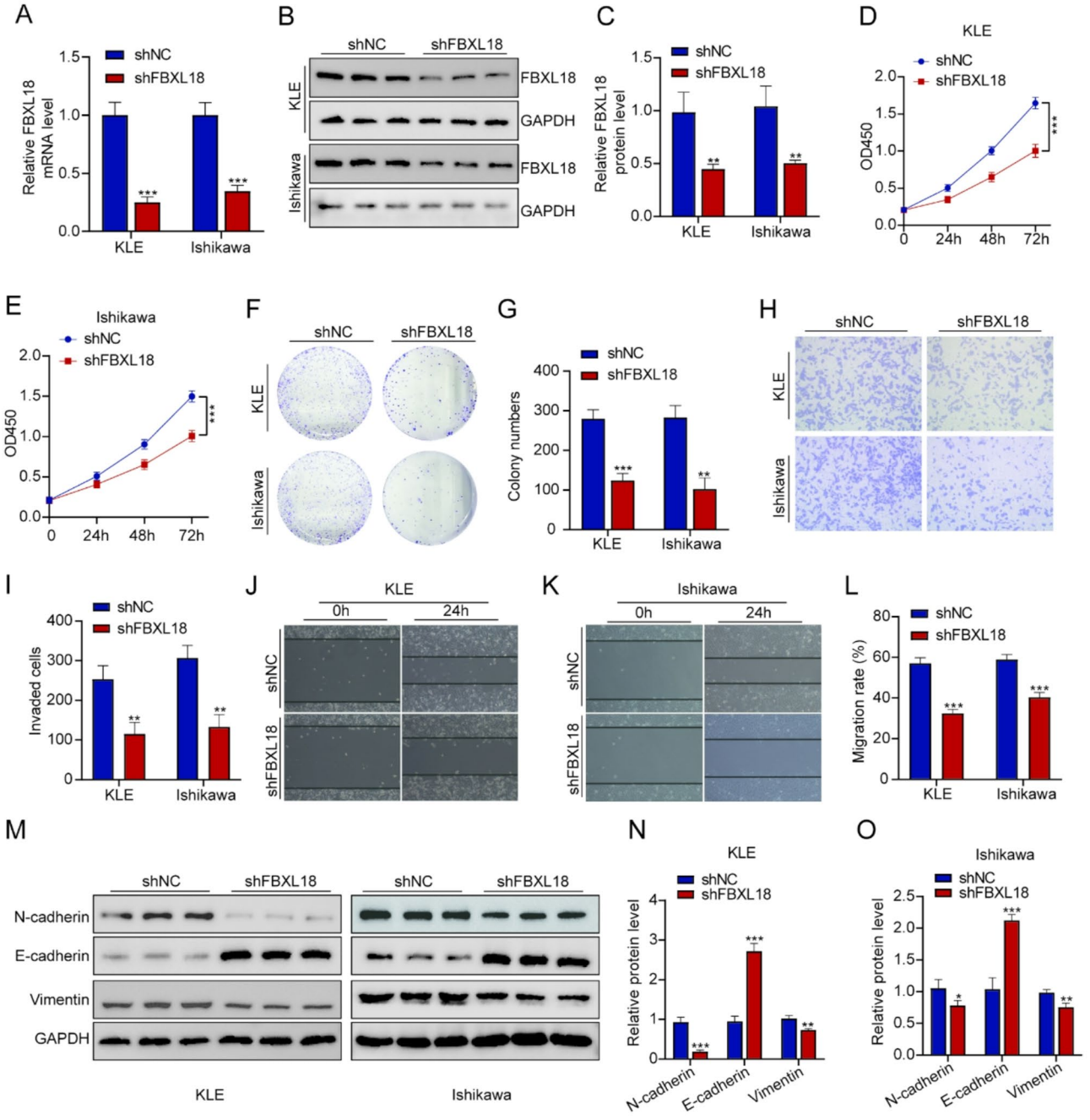

Fig. 2 Silence of FBXL18 impeded cell proliferation, migration, and invasion, and suppressed EMT in EC cells. (**A**) The mRNA levels of FBXL18 in EC cells of shNC and shFBXL18 groups were detected by qRT-PCR. (**B-C**) Western blot analysis of FBXL18 protein levels in EC cells of shNC and shFBXL18 groups, and quantitative analysis. (**D-G**) CCK-8 and colony formation assays were conducted to assess cell proliferation abilities in stably infected EC cells, and quantitative analyses. (**H-I**) Transwell invasion assay was used to evaluate invasiveness in EC cells after silencing FBXL18, and quantitative analysis. (**J-L**) Wound healing assay was employed to determine cell migration ability after silencing FBXL18 in KLE and Ishikawa cells, and quantitative analysis. (**M-O**) Western blot analysis of EMT related markers (N-cadherin, Vimentin, and E-cadherin) in EC cells of shNC and shFBXL18 groups, and quantitative analysis. **P* < 0.05; ***P* < 0.01; ****P* < 0.001

correlated with the proliferation maker *MKi67* (Fig. 4F) and multiple genes of the MAPK signaling pathway (Fig. 4G-T). Altogether, these analyses provided clues for the regulatory of FBXL18 on the activity of MAPK signaling pathway. Therefore, we further investigated the effect of FBXL18 knockdown or overexpression on MAPK signaling by detecting the protein levels of JNK, p-JNK, c-JUN, and p-c-JUN. As shown in Fig. 4U-W, silence of FBXL18 reduced the phosphorylation levels of JNK and c-JUN in KLE and Ishikawa cells. Conversely, enforced

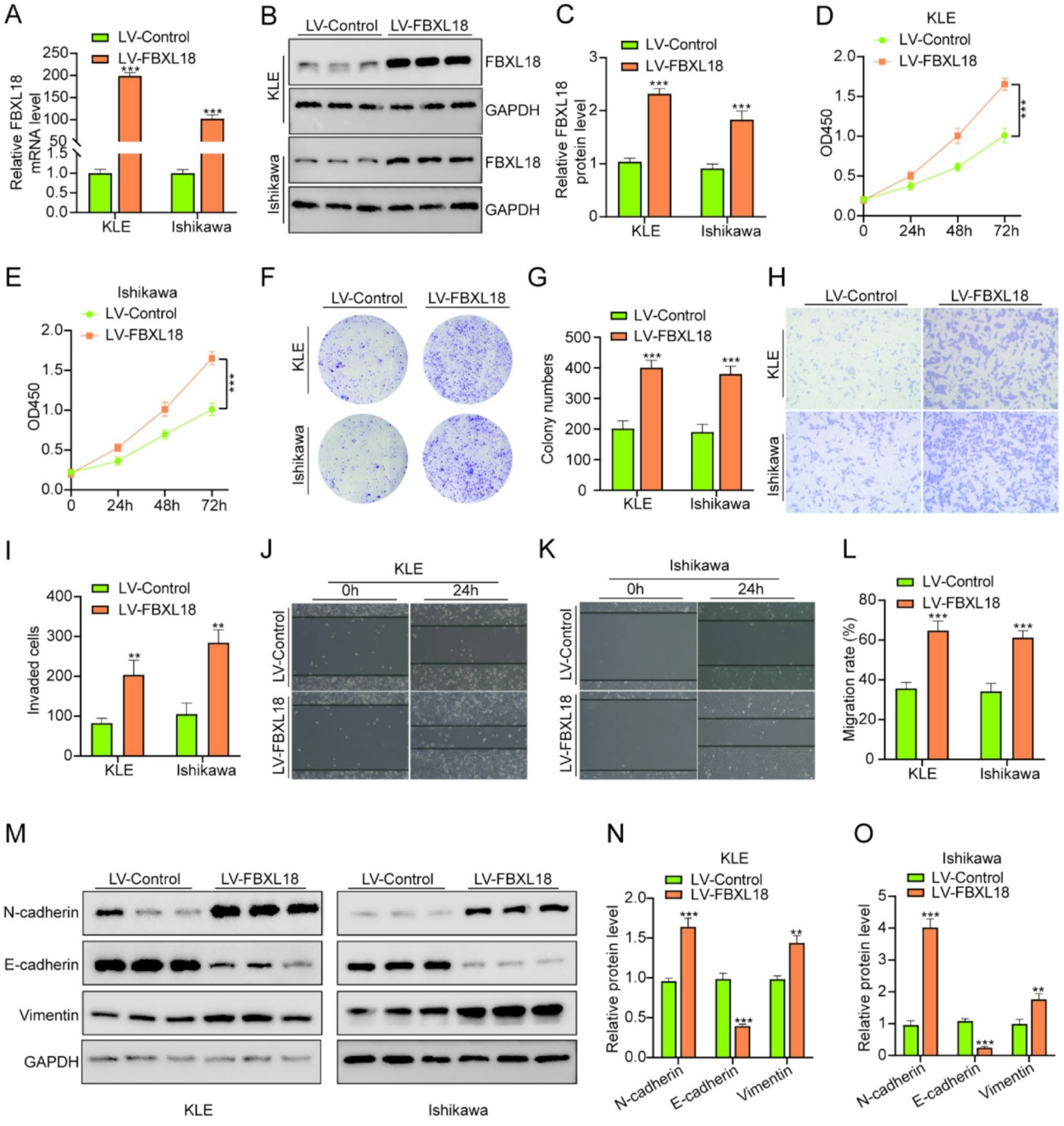

Fig. 3 Enforced expression of FBXL18 accelerated cell proliferation, migration, and invasion, and promoted EMT in EC cells. (**A**) The mRNA levels of FBXL18 in EC cells of LV-Control and LV-FBXL18 groups were detected by qRT-PCR. (**B-C**) Western blot analysis of FBXL18 protein levels in EC cells of LV-Control and LV-FBXL18 groups, and quantitative analysis. (**D-G**) CCK-8 and colony formation assays were conducted to assess cell proliferation abilities in stably infected EC cells, and quantitative analyses. (**H-I**) Transwell invasion assay was used to evaluate invasiveness in EC cells after overexpressing FBXL18, and quantitative analysis. (**J-L**) Wound healing assay was employed to determine cell migration ability after FBXL18 overexpression in KLE and Ishikawa cells, and quantitative analysis. (**M-O**) Western blot analysis of EMT related markers (N-cadherin, Vimentin, and E-cadherin) in EC cells of LV-Control and LV-FBXL18 groups, and quantitative analysis. *$P < 0.05$; **$P < 0.01$; ***$P < 0.001$

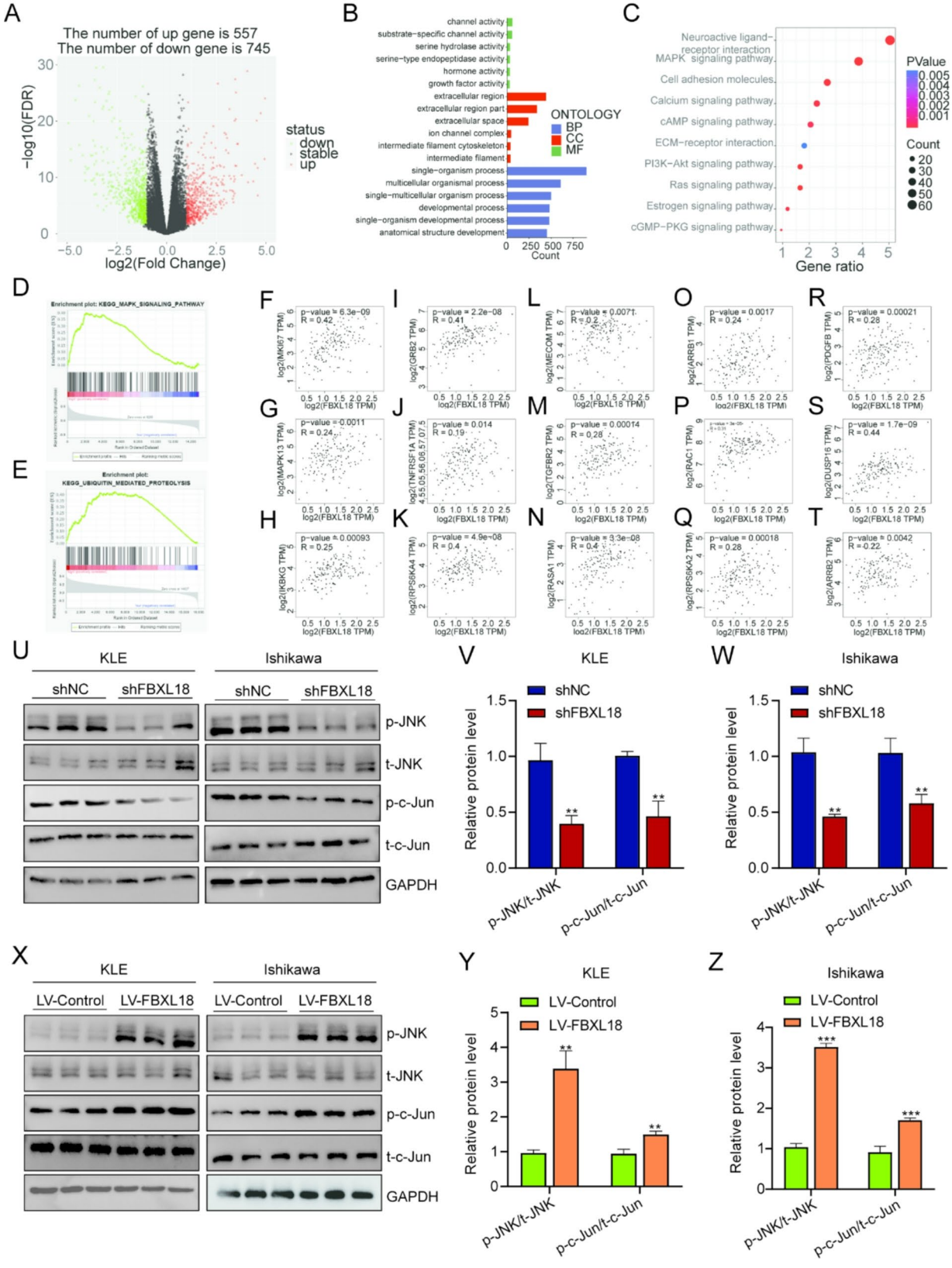

Fig. 4 (See legend on next page.)

(See figure on previous page.)

Fig. 4 FBXL18 positively regulated JNK signaling pathway in EC. (**A**) Volcano plot of FBXL18-related differentially expressed genes based on the RNA sequencing data of EC samples with high- and low-FBXL18 expression. (**B-C**) GO and KEGG enrichment analyses of FBXL18-related differentially expressed genes. (**D-E**) The results of GSEA revealed that MAPK and ubiquitin-mediated proteolysis were markedly enriched in $FBXL18^{High}$ group. (**F-T**) The Pearson's correlation analyses of FBXL18 and genes of the MAPK signaling pathway. (**U-W**) The protein levels of JNK, p-JNK, c-JUN, and p-c-JUN in EC cells after silencing FBXL18 were determined by western blot assay, and quantitative analysis. (**X-Z**) The protein levels of JNK, p-JNK, c-JUN, and p-c-JUN in EC cells after overexpressing FBXL18 were measured by western blot assay, and quantitative analysis. *$P < 0.05$; **$P < 0.01$; ***$P < 0.001$

expression of FBXL18 increased the levels of phosphorylated JNK and c-JUN in EC cells (Fig. 4X-Z). Additionally, SP600125, a small molecular inhibitor of JNK signaling, could partially reverse the promoting effect of FBXL18-overepxression on cell proliferation, migration, and invasion in EC cells (Supplementary Fig. 1A-F). Overall, these finding indicated that FBXL18 promoted the malignant behaviors in EC cells via activating MAKP/JNK signaling pathway.

FBXL18 targeted DUSP16 as a ubiquitination substrate

Given established role of FBXL18 in protein binding and stabilization, we tried to identify the direct substrates of FBXL18 in EC cells using the BioGRID database. DUSP16, one of the dual specificity phosphatases, was chosen for further investigation since it might be interacted with FBXL18, and due to its association with malignant characteristics in multiple tumors, as well as its vital role in regulating MAPK signaling [23]. For this purpose, we first evaluated the interaction between FBXL18 and DUSP16. As shown in Fig. 5A, IP assay confirmed the physical link of FBXL18 and DUSP16 in EC cells. Moreover, when co-overexpressing FBXL18-FLAG and DUSP16-HA in 293T cells, Co-IP results revealed that exogenous FBXL18 bound to DUSP16 (Fig. 5B). The results of cell immunofluorescence showed that FBXL18 and DUSP16 were co-localized in EC cells (Supplementary Fig. 2). Subsequently, we determined the mRNA and protein levels of DUSP16 in EC cells with altered FBXL18. The results showed that no alternations in DUSP16 mRNA levels were found in EC cells with either FBXL18 knockdown or overexpression (Fig. 5C-D). Western blot assay revealed that silencing FBXL18 led to the enhanced protein level of DUSP16 in EC cells (Fig. 5E-F), while DUSP16 protein level was decreased by FBXL18 overexpression (Fig. 5G-H). Therefore, we could conclude that FBXL18 might regulate the expression of DUSP16 through a post-transcriptional mechanism. Furthermore, we examined the mRNA and protein levels of DUSP16 in 12 paired EC and adjacent normal tissues. qRT-PCR results indicated that there was no significant difference in DUSP16 mRNA levels between EC and normal tissues (Supplementary Fig. 3A). However, Western blot analysis revealed that the protein level of DUSP16 was significantly lower in EC tissues compared to normal tissues (Supplementary Fig. 3B-C). These findings suggest that the downregulation of DUSP16 protein in EC tissues may be a consequence of FBXL18-mediated degradation rather than transcriptional regulation. Considering the function of FBXL18 as a E3 ligase, we tried to explore the influence of FBXL18 on the stability of DUSP16 in EC cells. In the CHX assay, our data illustrated that enforced FBXL18 resulted in faster DUSP16 degradation (Fig. 5I-J) and that silence of FBXL18 prolonged the half-life time of DUSP16 in EC cells (Fig. 5K-L), indicating that FBXL18 decreased the stability of DUSP16. Next, we determined whether FBXL18 regulated the ubiquitination of DUSP16. In *vivo* ubiquitination assay showed that the level of ubiquitinated DUSP16 was markedly reduced after silencing FBXL18 (Fig. 5M), while overexpression of FBXL18 increased the ubiquitination level of DUSP16 (Fig. 5N). Collectively, these results supported that FBXL18 targeted DUSP16 as a ubiquitination substrate and decreased the stability of DUSP16 in EC cells.

FBXL18 promoted cell malignancy via DUSP16-mediated activation of JNK signaling

To further explore whether FBXL18 mediated its tumorigenic function via DUSP16, we first investigated the effect of DUSP16 on the activation of JNK signaling in EC cells. As shown in Fig. 6A-C, knockdown of endogenous DUSP16 expression increased the levels of phosphorylated JNK and c-JUN. On the contrary, enforced expression of DUSP16 elicited significantly decreased phosphorylation levels of JNK and c-JUN in KLE and Ishikawa cells (Fig. 6D-F). These results suggested that DUSP16 was a vital determinant of JNK signaling in EC cells, which was consistent with previous researches [24]. To investigate whether DUSP16 mediated the effect of FBXL18 on the activation of JNK signaling pathway, DUSP16 was overexpressed or silenced in FBXL18-upregulated or downregulated EC cells. Western blot analysis illustrated that ectopic DUSP16 expression restored the expression of phosphorylated JNK and c-JUN, which were upregulated by FBXL18 overexpression (Fig. 6G-I). Similarly, the reduced expression of p-JNK and p-c-JUN resulting from FBXL18 knockdown was attenuated when DUSP16 was silenced in EC cells (Fig. 6J-L). Additionally, in *vitro* rescue experiments showed that silencing DUSP16 partially reversed the suppression of EC cell proliferation, migration and invasion caused by FBXL18 deletion (Supplementary Fig. 4A-B, **E-F**). Furthermore, upregulation of DUSP16 in EC cells alleviated FBXL18 overexpression-mediated enhanced

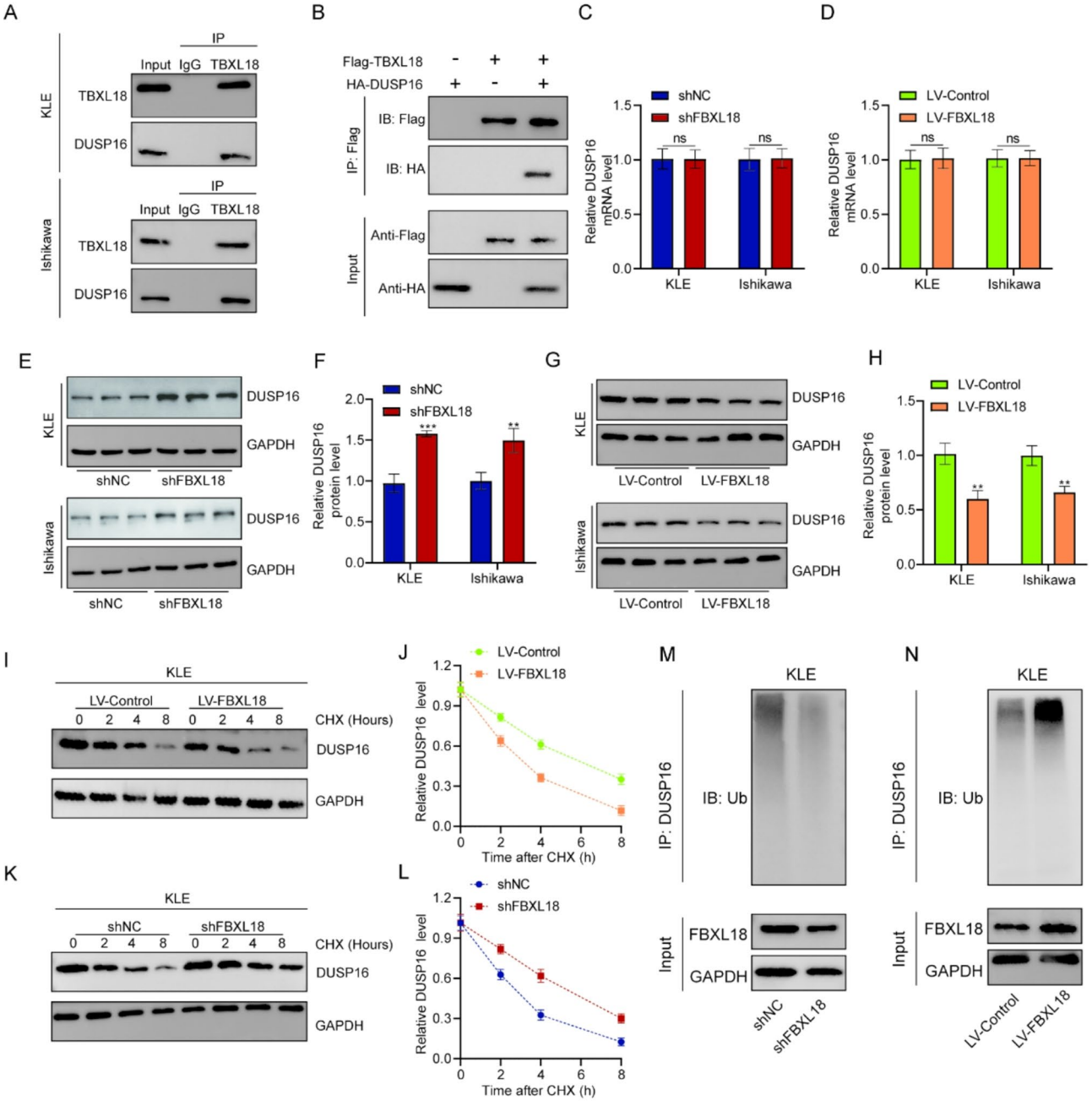

Fig. 5 FBXL18 targeted DUSP16 as a ubiquitination substrate. (**A-B**) The results of Co-IP and western blotting assays revealed the endogenous and exogenous interaction of FBXL18 and DUSP16. (**C-D**) qRT-PCR analysis of DUSP16 mRNA levels after silencing or overexpressing FBXL18 in KLE and Ishikawa cells. (**E-F**) Western blot analysis of DUSP16 protein level in EC cells of shNC and shFBXL18 groups, and quantitative analysis. (**G-H**) Western blot analysis of DUSP16 protein level in EC cells after overexpressing FBXL18, and quantitative analysis. (**I-J**) DUSP16 protein half-life in EC cells of LV-Control and LV-FBXL18 groups were evaluated by CHX chase assay. (**K-L**) Comparison of DUSP16 protein half-life in EC cells stably knockdown of FBXL18 and control cells. (**M-N**) The ubiquitination status of endogenous DUSP16 after silencing or overexpressing FBXL18 in EC cells were determined by immunoprecipitation and western blotting. *$P < 0.05$; **$P < 0.01$; ***$P < 0.001$

cell capacities of proliferation, migration, and invasion. (Supplementary Fig. 4C-D, **G-H**). Overall, these results supported that FBXL18 promoted malignant behaviors in EC cells via DUSP16-mediated activation of JNK signaling.

Silence of FBXL18 inhibited EC growth in vivo

To further examine the significance of FBXL18 deletion in EC cells in an in *vivo* setting, we developed a xenograft mouse model by subcutaneously injecting FBXL18-silenced (shFBXL18) or control (shNC) cells into immunodeficient mice, and monitored tumor growth

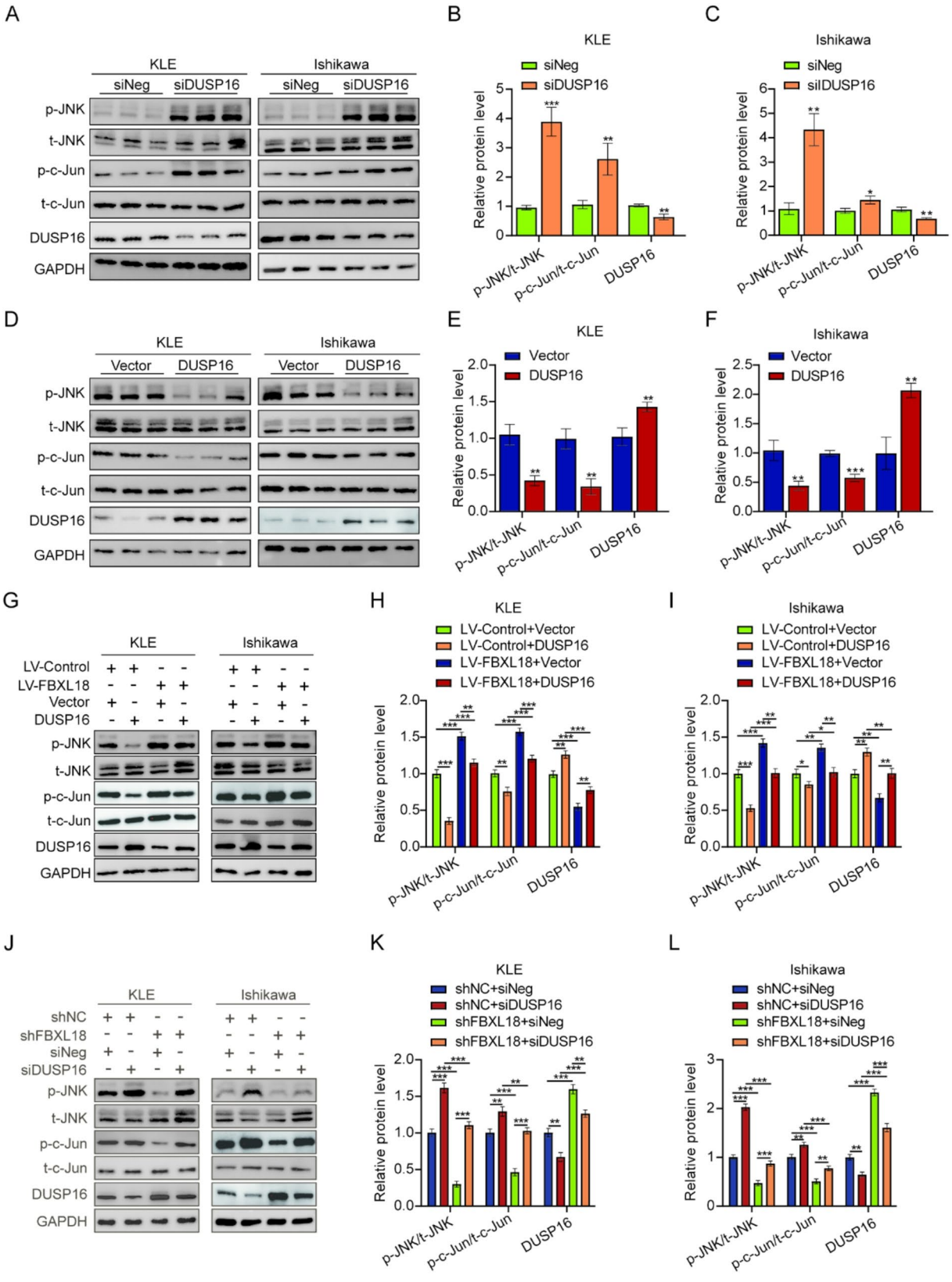

Fig. 6 (See legend on next page.)

(See figure on previous page.)

Fig. 6 FBXL18 promoted EC cell malignancy via DUSP16-mediated activation of JNK signaling. (**A-C**) Western blot analysis of DUSP16, JNK, p-JNK, c-JUN, and p-c-JUN levels in EC cells of siNeg and siDUSP16 groups, and quantitative analysis. (**D-F**) Western blot analysis of DUSP16, JNK, p-JNK, c-JUN, and p-c-JUN levels in EC cells after overexpressing DUSP16, and quantitative analysis. (**G-I**) Western blot analysis of DUSP16, JNK, p-JNK, c-JUN, and p-c-JUN levels in EC cells transfected with LV-Ctrl + Vector, LV-Ctrl + DUSP16, LV-FBXL18 + Vector, LV-FBXL18 + DUSP16, and quantitative analysis. (**J-L**) Western blot analysis of DUSP16, JNK, p-JNK, c-JUN, and p-c-JUN levels in EC cells transfected with shNC + siNeg, shNC + siDUSP16, shFBXL18 + siNeg, shFBXL18 + siDUSP16, and quantitative analysis. *$P < 0.05$; **$P < 0.01$; ***$P < 0.001$

every week until the mice being sacrificed. Subsequently, we randomly selected three samples from the two groups as representatives for subsequent Western blot experiments, and the tumor volume of these samples was close to the average value in the group, so as to ensure that these samples could represent the biological characteristics of the whole group. The results of qRT-PCR assays confirmed the downregulation of FBXL18 in tumor samples of shFBXL18 group compared to that in shNC group (Fig. 7F). The tumorigenicity assay results showed that silence of FBXL18 prominently led to decreased tumor volumes, sizes, and weights (Fig. 7A-C). Additionally, western blot analysis of xenograft displayed that the protein levels of N-cadherin, Vimentin, and phosphorylated JNK and c-JUN, were markedly decreased in shFBXL18 group when comparing to these in shNC group, while the expression of E-cadherin and DUSP16 were significantly enhanced (Fig. 7D-E). Besides, silence of FBXL18 did not alter the mRNA expression of DUSP16 in xenograft tumors (Fig. 7F). There results were consistent with the aforementioned findings in the *vitro* experiments, supporting that silence of FBXL18 inhibited EC growth in vivo, which was associated with increased protein level of DUSP16, and inactivation of JNK signaling.

Discussion

Ubiquitination, one of the most ubiquitous post-translational modification of proteins in mammalian cells, is a process tightly regulated by the dynamically balanced system, containing E3 ligases and deubiquitinases (DUBs), for controlling intracellular protein abundance [25–27]. In the ubiquitination cascade, certain E3 ligases could preciously identify substrate molecules, and then tag them with polyubiquitin chains, with the help of E1 activating and E2 conjugating enzymes [28]. These polyubiquitinated proteins were changed in intracellular localization, stability, trafficking, and function, or degraded by proteasomes or lysosomes [29–31]. On the contrary, the DUBs were responsible for the cleavage the ubiquitin chains from substrates and further regulated its stability [32]. Previous studies had shown that multiple E3 ligases and DUBs were frequently dysregulated in tumors and associated with oncogenesis, tumor progression, and response to therapies [33, 34]. FBXL18 belonged to the E3 ligases superfamily and was reported to play tumor-promoting roles in human cancers via regulating the ubiquitination of different targets. For example, Zhuang et al. [35]. found that FBXL18 promoted K63-linked ubiquitination of AKT to activate AKT signal, thus facilitating ovarian cancer tumorigenesis. Liu et al. [36]. revealed that FBXL18 suppressed apoptotic process in cervical cancer via mediating the ubiquitin-dependent proteasomal degradation of the pro-apoptotic protein FBXL7. Despite these studies, the involvement of FBXL18 in EC remains unknown.

In the present work, we showed the functional roles and underlying regulatory mechanism of FBXL18 in EC progression. We discovered that FBXL18 was highly expressed in EC tissues and cell lines through data mining methods and further experiments. Besides, higher expression of FBXL18 was associated with increased tumor stage and poor clinical outcome in EC patients. Plausibly, we envisaged that FBXL18 might be a promising prognostic biomarker for EC patients. The predictive performance of FBXL18 in EC needed to be further validated in multiple central and real-world cohorts. Moreover, we found that FBXL18 silencing suppressed EC cell proliferation, migration, and invasion in *vitro*, as well as impeded EC growth in *vivo*. Conversely, enforced expression of FBXL18 harbored the opposite effects. These data provided evidences for the tumorigenic role of FBXL18 in EC and presented a theoretical basis for the development of new therapeutic strategies by targeting FBXL18.

Afterwards, we focus on understanding the downstream pathways through which FBXL18 impacts the progression of EC. Using bioinformatic methods, we found that FBXL18-related differentially expressed genes were mainly involved in MAPK signaling in the KEGG enrichment analysis. Moreover, the results of GSEA also revealed that MAPK signaling were particularly enriched in $FBXL18^{High}$ groups compared to that in $FBXL18^{Low}$ group. Besides, *FBXL18* expression was positively correlated with multiple genes of the MAPK signaling pathway. These analyses provided a clue for the regulatory role of FBXL18 on MAPK signaling pathway in EC. The MAPK signaling is a ubiquitous signal transduction pathway that participates in all aspects of cellular processes such as cell proliferation, differentiation, stress responses and so on, and is frequently altered in human cancers [37, 38]. There are three major subfamilies of mitogen-activated protein kinases (MAPK) including extracellular signaling-regulated kinases (ERK), p38 MAPK, and the Jun N-terminal kinases (JNK) [39]. In the conventional MAPK cascade, external stimuli such as oxidative stress, inflammatory,

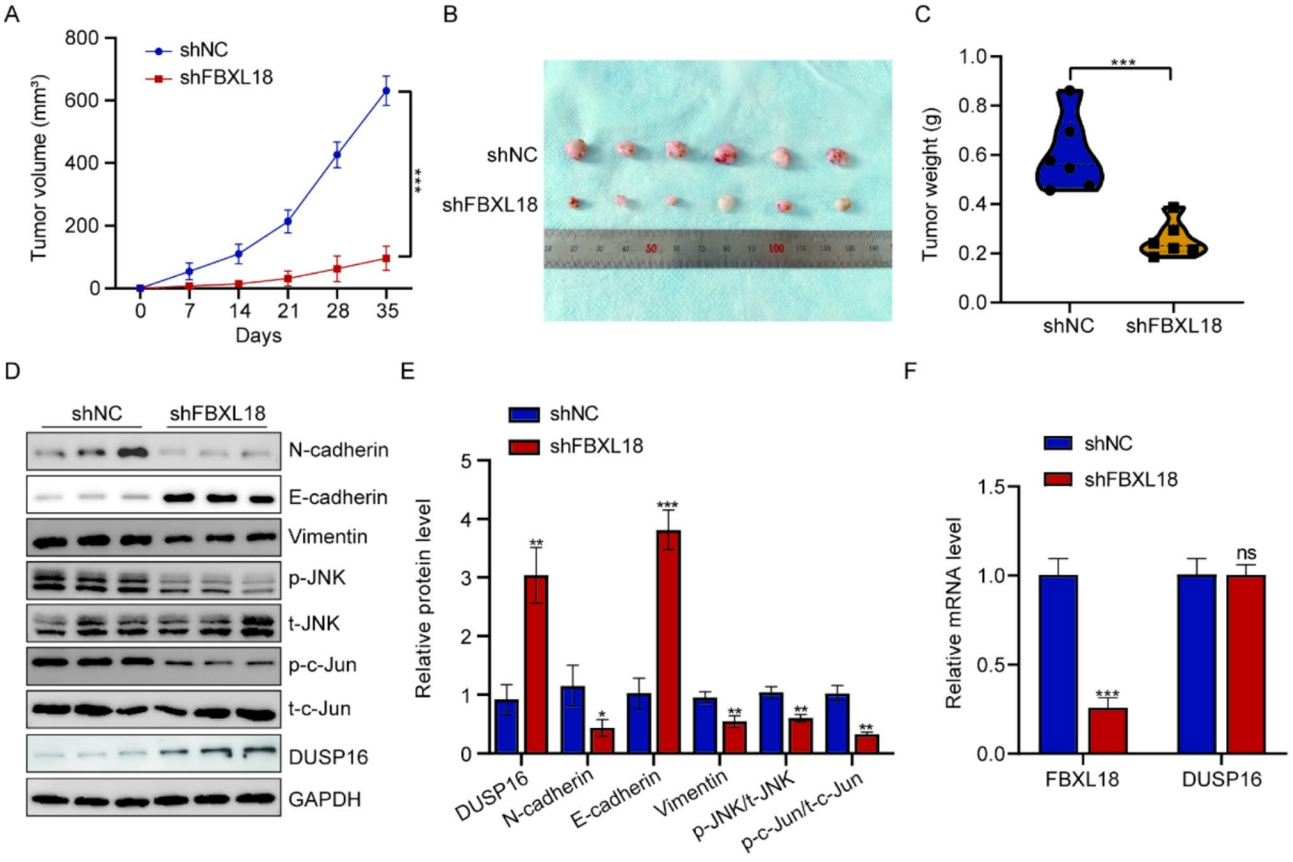

Fig. 7 Silence of FBXL18 inhibited EC growth in vivo. (**A**) Tumor volumes of shNC and shFBXL18 groups were determined at different defined time points. (**B**) Representative images of xenograft tumors in shNC and shFBXL18 groups. (**C**) Tumor weights of shNC and shFBXL18 groups were measured at the end point. (**E**) Western blot analysis of FBXL18, DUSP16, JNK, p-JNK, c-JUN, p-c-JUN, and EMT-related markers in tumor samples of shNC and shFBXL18 groups, and quantitative analysis. (**F**) qRT-PCR analysis of FBXL18 and DUSP16 in tumor samples of shNC and shFBXL18 groups. $^{*}P < 0.05$; $^{**}P < 0.01$; $^{***}P < 0.001$

and cytokine stimulation, were converted to a wide range of cellular responses by three major kinases: mitogen-activated protein kinase kinase kinase (MAPKKK), mitogen-activated protein kinase kinase (MAPKK), and MAPK [40]. Briefly, the MAPKKK phosphorylated MAPKK, which led to the activation of MAPK. Activated MAPK could bind to and phosphorylate various transcription factors such as c-JUN, p53, and MYC, and thus regulating cell cycle, proliferation, senescence, and apoptosis [41–43]. Previous studies had shown that the JNK pathway was frequently hyperactivated in solid tumors including cancers of liver, lung, brain, and colon [44–46]. Dysregulated JNK pathway participated in regulating cellular malignant behaviors in tumors and might be potential diagnostic or prognostic biomarkers, and therapeutic targets [47]. Therefore, we further evaluated the effect of FBXL18 on the activity of JNK pathway by determining the protein levels of p-JNK and its downstream target p-c-JUN. Our results illustrated that silence of FBXL18 decreased the phosphorylation levels of JNK and c-JUN, while enforced expression of FBXL18 increased the level of phosphorylated JNK and c-JUN, suggesting that FBXL18 positively regulated the activity of JNK/c-JUN signaling in EC. Furthermore, pharmacological inhibition of JNK signaling could reverse the promoting effect of FBXL18-overepxression on malignant behaviors in EC cells. Although JNK signaling pathway inhibitors such as SP600125 have shown some efficacy in partially reversing the malignant behavior of tumors caused by overexpression of FBXL18, the effect of JNK signaling inhibition may be limited to specific tumor behaviors and may have side effects. As an upstream regulator, FBXL18 not only mediates JNK signal activation through DUSP16, but also may affect other molecular pathways that have not been fully explored. Targeting FBXL18 may enable multi-target action, reducing the risk of compensatory resistance in tumor cells while reducing interference with JNK signaling in normal cells. Therefore, inhibition of FBXL18 may be a more effective and safer treatment strategy. Collectively, these results confirmed that FBXL18 promoted EC progression via activating JNK/c-Jun signaling.

Then, we sought to ascertain how FBXL18 regulated JNK pathway in EC. Considering that FBXL18 was an E3 ligase, we tried to identify the direct targets

of FBXL18 by analyzing its interacting proteins using BioGRID database. Of note, DUSP16, a dual specificity phosphatase, caught our attention since it might bind to FBXL18 and its abnormal expression was tightly associated with tumorigenesis and progression [48, 49]. Strikingly, DUSP16 was also previously reported to be a negative regulator of JNK [23, 50]. Therefore, we envisaged that DUSP16 was the direct substrate of FBXL18, and mediated its oncogenic potential. To confirmed this hypothesis, we first confirmed the physical interaction between FBXL18 and DUSP16 by co-immunoprecipitation assay. Moreover, our results illuminated that FBXL18 could negatively regulated DUSP16 protein levels in EC cells, but did not alter its mRNA levels, suggesting that FBXL18 regulated DUSP16 expression at a post-transcriptional level. Further experiments revealed that FBXL18 decreased the stability of DUSP16 and increased its ubiquitination levels. Besides, the reduced expression of p-JNK and p-c-JUN resulting from FBXL18 knockdown was attenuated when DUSP16 was silenced in EC cells. Additionally, silence of DUSP16 could partially reverse the proliferation and motility capabilities of FBXL18-deficient EC cells. Taken together, we could draw a conclusion that FBXL18 bound to DUSP16 and promoted its degradation to activate the JNK/c-JUN signaling pathway, therefore aggravating the tumorigenesis of EC.

There were some limitations in our study. First, the relationship between FBXL18 expression and clinicopathological characteristics of EC patients, as well as the correlation between FBXL18, DUSP16 and JNK/c-JUN in clinical samples need to be investigated. Another limitation is that we only identify FBXL18's abilities in malignant proliferation, invasion, and migration of EC cells, whether it influences cell cycle distribution, apoptosis, chemoresistance, and stemness should be further detected. Besides, the binding motif of FBXL18 and DUSP16 could be also explored.

In summary, we here successfully showcased the elevated expression, prognostic prediction performance, and the malignant tumor-promoting role of FBXL18 in EC. The novel mechanisms underlying this phenotype are that FBXL18 promotes the ubiquitination and degradation of DUSP16, and thus activated JNK/c-JUN signaling to facilitate EC progression. Our findings highlight the functional roles and associated mechanisms of FBXL18 in EC cell malignancy and provide valuable information for cancer prognosis evaluation and treatment in EC.

Supplementary Information

The online version contains supplementary material available at https://doi.org/10.1186/s12935-025-03808-9.

Supplementary Material 1

Acknowledgements
Not applicable.

Author contributions
All authors contributed to the study conception and design. Material preparation and the experiments were performed by Jie Pi and Yuzi Zhao. Data collection and analysis were performed by Yong Wang. The first draft of the manuscript was written by Jie Pi and Jing Yang. All authors commented on previous versions of the manuscript. All authors read and approved the final manuscript.

Funding
None.

Data availability
No datasets were generated or analysed during the current study.

Declarations

Ethics approval and consent to participate
The experiment with patient tissue specimens was authorized by the Ethics Committee of Renmin Hospital of Wuhan University. All animal experiments were approved by the Animal Care and Use Committee of Wuhan University Renmin Hospital.

Consent for publication
All authors have approved the publication of this study.

Competing interests
The authors declare no competing interests.

Received: 24 July 2024 / Accepted: 4 May 2025
Published online: 17 May 2025

References

1. Murali R, Soslow RA, Weigelt B. Classification of endometrial carcinoma: more than two types. Lancet Oncol. 2014;15(7):e268–278.
2. Huvila J, Pors J, Thompson EF, Gilks CB. Endometrial carcinoma: molecular subtypes, precursors and the role of pathology in early diagnosis. J Pathol. 2021;253(4):355–65.
3. Léon-Castillo A. Update in the molecular classification of endometrial carcinoma. Int J Gynecol Cancer. 2023;33(3):333–42.
4. Sung H, Ferlay J, Siegel RL, Laversanne M, Soerjomataram I, Jemal A, Bray F. Global Cancer statistics 2020: GLOBOCAN estimates of incidence and mortality worldwide for 36 cancers in 185 countries. CA Cancer J Clin. 2021;71(3):209–49.
5. Li J, Yang H, Zhang L, Zhang S, Dai Y. Metabolic reprogramming and interventions in endometrial carcinoma. Biomed Pharmacother. 2023;161:114526.
6. Crosbie EJ, Kitson SJ, McAlpine JN, Mukhopadhyay A, Powell ME, Singh N. Endometrial cancer. Lancet. 2022;399(10333):1412–28.
7. Concin N, Matias-Guiu X, Vergote I, Cibula D, Mirza MR, Marnitz S, Ledermann J, Bosse T, Chargari C, Fagotti A, et al. ESGO/ESTRO/ESP guidelines for the management of patients with endometrial carcinoma. Int J Gynecol Cancer. 2021;31(1):12–39.
8. Abu-Rustum N, Yashar C, Arend R, Barber E, Bradley K, Brooks R, Campos SM, Chino J, Chon HS, Chu C, et al. Uterine neoplasms, version 1.2023, NCCN clinical practice guidelines in oncology. J Natl Compr Canc Netw. 2023;21(2):181–209.
9. Dowdy SC. Improving oncologic outcomes for women with endometrial cancer: realigning our sights. Gynecol Oncol. 2014;133(2):370–4.
10. Turashvili G, Hanley K. Practical updates and diagnostic challenges in endometrial carcinoma. Arch Pathol Lab Med. 2024;148(1):78–98.
11. Hamilton SN, Tinker AV, Kwon J, Lim P, Kong I, Sihra S, Koebel M, Lee CH. Treatment and outcomes in undifferentiated and dedifferentiated endometrial carcinoma. J Gynecol Oncol. 2022;33(3):e25.
12. Kipreos ET, Pagano M. The F-box protein family. Genome Biol. 2000;1(5):Reviews3002.
13. Randle SJ, Laman H. F-box protein interactions with the hallmark pathways in cancer. Semin Cancer Biol. 2016;36:3–17.

14. Tekcham DS, Chen D, Liu Y, Ling T, Zhang Y, Chen H, Wang W, Otkur W, Qi H, Xia T, et al. F-box proteins and cancer: an update from functional and regulatory mechanism to therapeutic clinical prospects. Theranostics. 2020;10(9):4150–67.
15. Yan L, Lin M, Pan S, Assaraf YG, Wang ZW, Zhu X. Emerging roles of F-box proteins in cancer drug resistance. Drug Resist Updat. 2020;49:100673.
16. Yang Y, Xie Q, Hu C, Xu J, Chen L, Li Y, Luo C. F-box proteins and gastric cancer: an update from functional and regulatory mechanism to therapeutic clinical prospects. Int J Med Sci. 2024;21(8):1575–88.
17. Su J, Yin X, Zhou X, Wei W, Wang Z. The functions of F-box proteins in regulating the epithelial to mesenchymal transition. Curr Pharm Des. 2015;21(10):1311–7.
18. Zhang C, Pan G, Qin JJ. Role of F-box proteins in human upper Gastrointestinal tumors. Biochim Biophys Acta Rev Cancer. 2024;1879(1):189035.
19. Khan AQ, Al-Tamimi M, Uddin S, Steinhoff M. F-box proteins in cancer stemness: an emerging prognostic and therapeutic target. Drug Discov Today. 2021;26(12):2905–14.
20. Yu HQ, Li F, Xiong H, Fang L, Zhang J, Bie P, Xie CM. Elevated FBXL18 promotes RPS15A ubiquitination and SMAD3 activation to drive HCC. Hepatol Commun 2023, 7(7).
21. Yoshida A, Choi J, Jin HR, Li Y, Bajpai S, Qie S, Diehl JA. Fbxl8 suppresses lymphoma growth and hematopoietic transformation through degradation of Cyclin D3. Oncogene. 2021;40(2):292–306.
22. Colas E, Pedrola N, Devis L, Ertekin T, Campoy I, Martínez E, Llauradó M, Rigau M, Olivan M, Garcia M, et al. The EMT signaling pathways in endometrial carcinoma. Clin Transl Oncol. 2012;14(10):715–20.
23. Lee S, Syed N, Taylor J, Smith P, Griffin B, Baens M, Bai M, Bourantas K, Stebbing J, Naresh K, et al. DUSP16 is an epigenetically regulated determinant of JNK signalling in Burkitt's lymphoma. Br J Cancer. 2010;103(2):265–74.
24. Hoornaert I, Marynen P, Goris J, Sciot R, Baens M. MAPK phosphatase DUSP16/MKP-7, a candidate tumor suppressor for chromosome region 12p12-13, reduces BCR-ABL-induced transformation. Oncogene. 2003;22(49):7728–36.
25. Han S, Wang R, Zhang Y, Li X, Gan Y, Gao F, Rong P, Wang W, Li W. The role of ubiquitination and deubiquitination in tumor invasion and metastasis. Int J Biol Sci. 2022;18(6):2292–303.
26. Cockram PE, Kist M, Prakash S, Chen SH, Wertz IE, Vucic D. Ubiquitination in the regulation of inflammatory cell death and cancer. Cell Death Differ. 2021;28(2):591–605.
27. Dewson G, Eichhorn PJA, Komander D. Deubiquitinases in cancer. Nat Rev Cancer. 2023;23(12):842–62.
28. Cruz Walma DA, Chen Z, Bullock AN, Yamada KM. Ubiquitin ligases: guardians of mammalian development. Nat Rev Mol Cell Biol. 2022;23(5):350–67.
29. Sampson C, Wang Q, Otkur W, Zhao H, Lu Y, Liu X, Piao HL. The roles of E3 ubiquitin ligases in cancer progression and targeted therapy. Clin Transl Med. 2023;13(3):e1204.
30. Spano D, Catara G. Targeting the Ubiquitin-Proteasome system and recent advances in Cancer therapy. Cells 2023, 13(1).
31. Sun T, Liu Z, Yang Q. The role of ubiquitination and deubiquitination in cancer metabolism. Mol Cancer. 2020;19(1):146.
32. Ren J, Yu P, Liu S, Li R, Niu X, Chen Y, Zhang Z, Zhou F, Zhang L. Deubiquitylating enzymes in Cancer and immunity. Adv Sci (Weinh). 2023;10(36):e2303807.
33. Zhou X, Sun SC. Targeting ubiquitin signaling for cancer immunotherapy. Signal Transduct Target Ther. 2021;6(1):16.
34. Basu B, Ghosh MK. Ubiquitination and deubiquitination in the regulation of epithelial-mesenchymal transition in cancer: shifting gears at the molecular level. Biochim Biophys Acta Mol Cell Res. 2022;1869(7):119261.
35. Zhuang Y, Xue J, Qiu X, Zhu Y, Lv J, Xia F. FBXL18 is required for ovarian cancer cell proliferation and migration through activating AKT signaling. Am J Transl Res. 2024;16(5):1977–90.
36. Liu Y, Lear T, Zhao Y, Zhao J, Zou C, Chen BB, Mallampalli RK. F-box protein Fbxl18 mediates polyubiquitylation and proteasomal degradation of the pro-apoptotic SCF subunit Fbxl7. Cell Death Dis. 2015;6(2):e1630.
37. Park HB, Baek KH. E3 ligases and deubiquitinating enzymes regulating the MAPK signaling pathway in cancers. Biochim Biophys Acta Rev Cancer. 2022;1877(3):188736.
38. Anjum J, Mitra S, Das R, Alam R, Mojumder A, Emran TB, Islam F, Rauf A, Hossain MJ, Aljohani ASM, et al. A renewed concept on the MAPK signaling pathway in cancers: polyphenols as a choice of therapeutics. Pharmacol Res. 2022;184:106398.
39. Yu B, Zhang Y, Wang T, Guo J, Kong C, Chen Z, Ma X, Qiu T. MAPK signaling pathways in hepatic ischemia/reperfusion injury. J Inflamm Res. 2023;16:1405–18.
40. Lee S, Rauch J, Kolch W. Targeting MAPK signaling in cancer: mechanisms of drug resistance and sensitivity. Int J Mol Sci 2020, 21(3).
41. Morgos DT, Stefani C, Miricescu D, Greabu M, Stanciu S, Nica S, Stanescu S, II, Balan DG, Balcangiu-Stroescu AE, Coculescu EC et al. Targeting PI3K/AKT/mTOR and MAPK signaling pathways in gastric Cancer. Int J Mol Sci 2024, 25(3).
42. Sala-Gaston J, Costa-Sastre L, Pedrazza L, Martinez-Martinez A, Ventura F, Rosa JL. Regulation of MAPK signaling pathways by the large HERC ubiquitin ligases. Int J Mol Sci 2023, 24(5).
43. Kciuk M, Gielecińska A, Budzinska A, Mojzych M, Kontek R. Metastasis and MAPK pathways. Int J Mol Sci 2022, 23(7).
44. Pua LJW, Mai CW, Chung FF, Khoo AS, Leong CO, Lim WM, Hii LW. Functional roles of JNK and p38 MAPK signaling in nasopharyngeal carcinoma. Int J Mol Sci 2022, 23(3).
45. Yang F, Li M, Xu D, Jiang Z, Jiang H, Xiao Y, Mei C, Yang M, Chen C, Zhou B, et al. Inhibition of JNK/c-Jun-ATF2 overcomes cisplatin resistance in liver Cancer through down-Regulating Galectin-1. Int J Biol Sci. 2023;19(8):2366–81.
46. Bai Y, Liu X, Qi X, Liu X, Peng F, Li H, Fu H, Pei S, Chen L, Chi X, et al. PDIA6 modulates apoptosis and autophagy of non-small cell lung cancer cells via the MAP4K1/JNK signaling pathway. EBioMedicine. 2019;42:311–25.
47. Wagner EF, Nebreda AR. Signal integration by JNK and p38 MAPK pathways in cancer development. Nat Rev Cancer. 2009;9(8):537–49.
48. Low HB, Wong ZL, Wu B, Kong LR, Png CW, Cho YL, Li CW, Xiao F, Xin X, Yang H, et al. DUSP16 promotes cancer chemoresistance through regulation of mitochondria-mediated cell death. Nat Commun. 2021;12(1):2284.
49. Zhang H, Zheng H, Mu W, He Z, Yang B, Ji Y, Hui L. DUSP16 ablation arrests the cell cycle and induces cellular senescence. Febs J. 2015;282(23):4580–94.
50. Nizamutdinova IT, Kim YM, Lee JH, Chang KC, Kim HJ. MKP-7, a negative regulator of JNK, regulates VCAM-1 expression through IRF-1. Cell Signal. 2012;24(4):866–72.

Publisher's note